Journal of Communications Technology and Electronics, Vol. 49, No. 2, 2004, pp. 139–153. Translated from Radiotekhnika i Elektronika, Vol. 49, No. 2, 2004, pp. 156–170.

THEORY AND METHODS OF SIGNAL PROCESSING

One-Stage Estimation of the Position of a Radio Source by a Passive System Consisting of Narrow-Base Subsystems

A. V. Dubrovin and Yu. G. Sosulin

Received January 9, 2003

Abstract—An optimal algorithm for the one-stage estimation of the radiator position by a passive system consisting of narrow-base subsystems was developed. A comparative analysis of one-stage and direction-finding (two-stage) methods was carried out using both the Cramér–Rao matrix bound and computer simulation. It was shown that one-stage and direction-finding methods offer equal accuracies of measuring the radiator coordinates if the signal-to-noise ratio exceeds some threshold value. It was revealed that, for low values of the signal-to-noise ratio, the one-stage method is far more resistant to abnormal errors than the direction-finding method.

1. INTRODUCTION

In this work, we analyze a passive system for the one-stage determination of the radiator position. The system consists of narrow-base subsystems (NBSs) and a central processing station (CPS) (see Fig. 1). A narrow-base subsystem contains reception points (RPs) spaced by a distance comparable to the wavelength of the received signal and substantially less than the distances to the radiator, digital signal processing unit, and subsystem ensuring the data exchange between the NBS and the CPS. By the reception point, we mean an antenna with a circular pattern whose signal is amplified, selected in the chosen frequency band, and converted to an intermediate frequency (if this is required by the design of the receiving section (RS)). The closest analog of the proposed system is a direction-finding system for determining coordinates of a radiator using the phase-comparison method for measuring bearing angles. The main difference between the one-stage estimation system studied in this paper and the direction-finding system lies in the fact that, in this case, estimated parameters are the radiator coordinates, and direct measurements of intermediate parameters (bearing angles) are not carried out.

The one-stage method for estimation of the radiator coordinates by a wide-base passive system was analyzed in [1]. It is significant that implementation of this method requires at least three RPs spaced by distances comparable to the distance to the radiator. Placing the RPs onboard such carriers as a helicopter or an airplane makes this system expensive. At the same time, the method proposed in this work can be implemented with a single carrier moving in space, which is undoubtedly an attractive way of reducing the cost of the radiator-position finding system.

2. FORMULATION OF THE PROBLEM

Let us have a radiator (R) generating narrowband signal $s(t)$ in a frequency band ranging from f_1 to f_2. This signal is received by N narrow-base subsystems. Each (nth) NBS contains M_n spaced RPs. Accordingly, the entire measuring system contains $\sum_{n=1}^{N} M_n$ RPs. Signals received at the RPs are mixed with noises $\xi_{nm_n}(t)$ ($n = \overline{1, N}$ and $m_n = \overline{1, M_n}$). The signal and noises are stationary, ergodic, and mutually independent Gaussian processes with zero mean.

Let us assume that delays between signals received by the spaced RPs only result from their mutual positions in space. At the same time, there are factors creating additional distortions during the signal reception that cannot be rigorously taken into account (multiple reflections from nearby structures, differences in parameters of antennas and feeders, etc.). We assume that these distortions are sufficiently small to allow

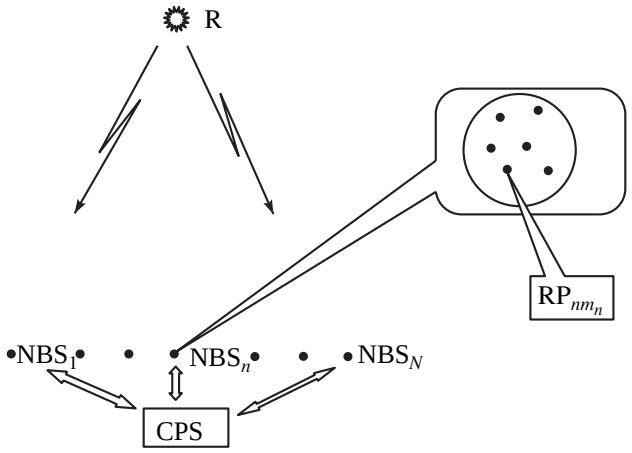

Fig. 1.

their approximate consideration by increasing the power of noise components $\xi_{nm_n}(t)$.

We assume that observation time T_o is substantially larger than the widths of correlation functions (correlation lengths) of both the signal and the noises as well as the maximum possible delay between signals. We also assume that RPs of the nth NBS receive the nth sample of desired signal $s(t)$ that does not overlap the kth sample ($n \neq k$, where $n, k = \overline{1, N}$). This assumption is valid when several NBSs are formed using one NBS moving in space and the error in the time synchronization of different NBSs substantially exceeds correlation lengths of both the signal and the noise.

Thus, the model of processes observed in NBSs can be written as

$$u_{nm_n}(t) = s_{nm_n}(t) + \xi_{nm_n}(t), \quad (1)$$

where $s_{nm_n}(t) = \sqrt{a_n}\, s_n(t - \tau_{nm_n})$ is the desired signal at the input of RP_{nm_n} (the m_nth RP of the nth NBS), a_n is the amplitude factor determined by the power attenuation coefficient for signal $s_n(t)$ passing from radiator R to the nth NBS, $\tau_{nm_n}(\mathbf{r}) = R_{nm_n}(\mathbf{r})/c$ is the time in which signal $s(t)$ travels from R to RP_{nm_n}, $R_{nm_n}(\mathbf{r}) = \sqrt{(\mathbf{r}_{nm_n} - \mathbf{r})^T(\mathbf{r}_{nm_n} - \mathbf{r})}$ is the distance from the radiator to RP_{nm_n} (where $n = \overline{1, N}$ and $m_n = \overline{1, M_n}$), c is the signal propagation speed, $\mathbf{r} = \|X_\mathrm{R}, Y_\mathrm{R}, Z_\mathrm{R}\|^T$ are the radiator coordinates, $\mathbf{r}_{nm_n} = \|X_{nm_n}, Y_{nm_n}, Z_{nm_n}\|^T$ are coordinates of the RP_{nm_n}, and T denoted the operation of transposition.

In the frequency domain, formula (1) is replaced by $U_{nm_n}(f) = S_{nm_n}(f) + \Xi_{nm_n}(f)$, where

$$U_{nm_n}(f) = \int_{-\infty}^{+\infty} u_{nm_n}(t)\exp(-j2\pi ft)dt = F(u_{nm_n}(t));$$
$$S_{nm_n}(f) = F(s_{nm_n}(t));$$

$\Xi_{nm_n}(f) = F(\xi_{nm_n}(f))$, and F is the Fourier transform operator.

3. SYNTHESIS OF THE ONE-STAGE ALGORITHM FOR ESTIMATION OF THE RADIATOR COORDINATES

We will seek an estimate of the radiator coordinates using the maximum likelihood method. Let us assume that we know covariance functions of signal $s(t)$ and noise $\xi_{nm_n}(t)$,

$$\mathrm{K}_s(\tau) = \mathrm{M}[s_n(t)s_n(t-\tau)] = \mathrm{M}[s_l(t)s_l(t-\tau)],$$
$$\mathrm{K}_{\xi nm_n}(\tau) = \mathrm{M}[\xi_{nm_n}(t)\xi_{nm_n}(t-\tau)],$$
$$\mathrm{M}[s_n(t)] = 0, \quad \mathrm{M}[s_n(t)s_l(t-\tau)] = 0, \quad \mathrm{M}[\xi_{nm_n}(t)] = 0$$
$$(n, l = \overline{1, N},\ n \neq l,\ m_n = \overline{1, M_n}),$$

and their power spectral densities,

$$G_s(f) = \int_{-\infty}^{+\infty} \mathrm{K}_s(\tau)\exp(-j2\pi f\tau)d\tau$$

and

$$G_{\xi nm_n}(f) = \int_{-\infty}^{+\infty} \mathrm{K}_{\xi nm_n}(\tau)\exp(-j2\pi f\tau)d\tau.$$

Since the signal and the noise are independent quantities, the covariance matrix of the observed process is

$$\mathrm{K}_{u_{nm_n}u_{nl_n}}(\tau) = \mathrm{M}[u_{nm_n}(t)u_{nl_n}(t-\tau)]$$
$$= a_n\mathrm{K}_s[\tau - \tau_{nm_n}(\mathbf{r}) + \tau_{nl_n}(\mathbf{r})] + \delta_{nm_nnl_n}\mathrm{K}_{\xi nm_n}(\tau)$$
$$(m_n = \overline{1, M_n},\ l_n = \overline{1, M_n}), \quad (2)$$
$$\mathrm{K}_{u_{nm_n}u_{kl_k}}(\tau) = \mathrm{M}[u_{nm_n}(t)u_{kl_k}(t-\tau)] = 0$$
$$(n \neq k,\ n,k = \overline{1, N},\ m_n = \overline{1, M_n},\ l_k = \overline{1, M_k}),$$

where $\delta_{nm_nnl_n} = 1$ for $m_n = l_n$ and $\delta_{nm_nnl_n} = 0$ for $m_n \neq l_n$.

Using formulas (2), we can write expressions for spectral densities [2] of analyzed signals and noises:

$$G_{u_{nm_n}u_{nl_n}}(f) = \int_{-\infty}^{+\infty} \mathrm{K}_{u_{nm_n}u_{nl_n}}(\tau)\exp(-j2\pi f\tau)d\tau$$
$$= a_nG_s(f)\exp\{-j2\pi f(\tau_{nm_n} - \tau_{kl_k})\} + \delta_{nm_nnl_n}G_{\xi nm_n}(f), \quad (3)$$
$$G_{u_{nm_n}u_{kl_k}}(f) = \int_{-\infty}^{+\infty} \mathrm{K}_{u_{nm_n}u_{kl_k}}(\tau)\exp(-j2\pi f\tau)d\tau = 0.$$

Thus, cross-spectral density $G_{u_{nm_n}u_{nl_n}}(f)$ and cross-covariance function $\mathrm{K}_{u_{nm_n}u_{nl_n}}(\tau)$ are known to within amplitude factors a_n and delay $\tau_{nm_n}(\mathbf{r}) - \tau_{kl_k}(\mathbf{r})$ depending on radiator coordinates $\mathbf{r}$.

Let us write the likelihood function (LF) taking into account that observation time T_o is the same for all NBSs. We assume also that time T_o is far larger than

maximum possible delay $\tau_{n\max}$. In this case, the LF takes the form

$$P(\mathbf{U}|\mathbf{r}, \mathbf{a}) = C_{\mathrm{n}}(\mathbf{a})\exp\left[-\frac{1}{2}\mathbf{U}^T\mathbf{G}^{-1}(\mathbf{r}, \mathbf{a})\mathbf{U}^*\right], \quad (4)$$

where $C_{\mathrm{n}}(\mathbf{a}) = (2\pi)^{-I\mathcal{M}/2}|\mathbf{G}(\mathbf{r}, \mathbf{a})|^{-1/2}$ is the normalizing factor depending (as will be shown below) only on vector $\mathbf{a} = \|a_1, \ldots, a_N\|^T$,

$$\mathbf{U} = \left\|\mathbf{U}^T(0), \ldots, \mathbf{U}^T(I-1)\right\|^T;$$
$$\mathbf{U}(i) = \left\|\mathbf{U}_1^T(i), \ldots, \mathbf{U}_N^T(i)\right\|^T;$$

$$\mathbf{U}_n(i) = \left\|\mathcal{U}_{n1}(i), \ldots, \mathcal{U}_{nM_n}(i)\right\|^T$$
$$(i = \overline{0, I-1} \text{ and } n = \overline{1, N});$$

$$\mathcal{U}_{nm_n}(i) = \frac{1}{T_{\mathrm{o}}}\int_{-T_{\mathrm{o}}/2}^{+T_{\mathrm{o}}/2} u_{nm_n}(t)\exp(-j2\pi i f_\Delta t)dt;$$
$$m_n = \overline{1, M_n}; \quad i = \overline{0, I-1};$$

I is the number of frequency components in the signal spectrum, $f_\Delta = \frac{1}{T_{\mathrm{o}}}$, $\mathbf{G}(\mathbf{r}, \mathbf{a}) = \mathrm{M}(\boldsymbol{U}^*\boldsymbol{U}^T) = \mathrm{diag}(\mathbf{G}_n(i))$ is the $I\mathcal{M}\times I\mathcal{M}$ covariance matrix ($\mathcal{M} = \sum_{n=1}^N M_n$ is the total number of RPs) consisting of $IN \times IN$ submatrices of which nonzero ones are only $M_n \times M_n$ submatrices $\mathbf{G}_n(i)$ situated on the diagonal, $\mathbf{G}_n(i) = \mathbf{D}_n^*(i)(a_n\mathcal{G}_s(i)\mathbf{1}_n + \mathbf{G}_{\xi n}(i))\mathbf{D}_n(i)) = \mathrm{diag}(a_n\mathcal{G}_s(i)\mathbf{D}_n^*(i)\times(\mathbf{1}_n + \mathbf{C}_n(i))\mathbf{D}_n(i))$, $\mathbf{1}_n$ is the $M_n \times M_n$ submatrix with all elements equal to unity, $\mathbf{G}_{\xi n}(i) = \mathrm{diag}(\mathcal{G}_{\xi nm_n}(i))$, $\mathbf{D}_n(i) = \mathrm{diag}(\exp(-j2\pi i f_\Delta \tau_{nm_n}))$, $\mathbf{C}_n(i) = \mathrm{diag}\left(\frac{\mathcal{G}_{\xi nm_n}(i)}{\mathcal{G}_s(i)a_n}\right)$ ($m_n = \overline{1, M_n}$) are $M_n \times M_n$ diagonal matrices in which only (m_n, m_n)th diagonal elements take nonzero values, $\mathcal{G}_{\xi nm_n}(i) = \frac{1}{T_{\mathrm{o}}}G_{\xi nm_n}(if_\Delta)$, and $\mathcal{G}_s(i) = \frac{1}{T_{\mathrm{o}}}G_s(if_\Delta)$.

The inverse covariance matrix is

$$\mathbf{G}^{-1}(\mathbf{r}, \mathbf{a}) = \mathrm{diag}(\mathbf{G}_n^{-1}(i)). \quad (5)$$

If we take into account that, after the inversion of $N \times N$ "direct" matrix $\mathbf{Z} = \mathbf{1} + \mathbf{X}$, where $\mathbf{X}$ is the diagonal matrix with elements $X_1, \ldots, X_N$, we obtain inverse matrix $\mathbf{Z}^{-1} = \mathbf{X}^{-1}(\mathbf{E} - \delta\mathbf{1}\mathbf{X}^{-1})$, where $\mathbf{E}$ is the identity matrix and $\delta = (1 + 1/X_1 + 1/X_2 + \ldots + 1/X_N)^{-1}$, then we find that

$$\mathbf{G}_n^{-1}(i) = a_n^{-1}\mathcal{G}_s^{-1}(i)\mathbf{D}_n^*(i)\mathbf{C}_n^{-1}(i)$$
$$\times\left(\mathbf{E}_n - \left(1 + \sum_{m_n=1}^{M_n}\frac{a_n\mathcal{G}_s(i)}{\mathcal{G}_{\xi nm_n}(i)}\right)^{-1}\mathbf{1}_n\mathbf{C}_n^{-1}(i)\right)\mathbf{D}_n(i)$$
$$= \mathbf{D}_n^*(i)\left(\mathbf{G}_{\xi n}^{-1}(i)\right.$$
$$\left. - a_n\mathcal{G}_s(i)\mathbf{Q}_n(i)\left(1 + \sum_{m_n=1}^{M_n}\frac{a_n\mathcal{G}_s(i)}{\mathcal{G}_{\xi nm_n}(i)}\right)^{-1}\right)\mathbf{D}(i), \quad (6)$$

where submatrix $\mathbf{Q}_n(i)$ consists of elements $\mathcal{Q}_{m_n l_n}(i) = \mathcal{G}_{\xi nm_n}^{-1}(i)\mathcal{G}_{\xi nl_n}^{-1}(i)$ $(m_n, l_n = \overline{1, M_n})$; $\mathbf{G}_{\xi n}^{-1}(i) = \mathrm{diag}(\mathcal{G}_{\xi nm_n}^{-1}(i))$; and $\mathbf{E}_n$ is the $M_n \times M_n$ identity matrix.

Then,

$$P(\mathbf{U}|\mathbf{r}, \mathbf{a}) = C_{\mathrm{n}}(\mathbf{a})$$
$$\times\exp\left\{-\frac{1}{2}\left[\sum_{n=1}^N (J_{0n} - J_{1n}(a_n) - 2\mathrm{Re}(J_{2n}(\mathbf{r}, a_n)))\right]\right\}, \quad (7)$$

where $2\mathrm{Re}(J_{2n}(\mathbf{r}, a_n)) = J_{2n}(\mathbf{r}, a_n) + J_{2n}^*(\mathbf{r}, a_n)$;

$$J_{0n} = \sum_{m_n=1}^{M_n}\sum_{i=0}^{I-1}\mathcal{G}_{\xi nm_n}^{-1}(i)\mathcal{U}_{nm_n}(i)\mathcal{U}_{nm_n}^*(i);$$

$$J_{1n}(a_n) = \sum_{m_n=1}^{M_n}\sum_{i=0}^{I-1}\mathcal{U}_{nm_n}(i)\mathcal{U}_{nm_n}^*(i)$$
$$\times\frac{a_n\mathcal{G}_s(i)}{\mathcal{G}_{\xi nm_n}^2(i)}\left(1 + \sum_{m_n=1}^{M_n}\frac{a_n\mathcal{G}_s(i)}{\mathcal{G}_{\xi nm_n}(i)}\right)^{-1};$$

$$J_{2n}(\mathbf{r}, a_n) = \sum_{l_n=1}^{M_n-1}\sum_{m_n=l_n+1}^{M_n}\sum_{i=0}^{I-1}\frac{a_n\mathcal{G}_s(i)}{\mathcal{G}_{\xi nm_n}(i)\mathcal{G}_{\xi nl_n}(i)}$$
$$\times\left(1 + \sum_{m_n=1}^{M_n}\frac{a_n\mathcal{G}_s(i)}{\mathcal{G}_{\xi nm_n}(i)}\right)^{-1}\mathcal{U}_{nm_n}(i)\mathcal{U}_{nl_n}^*(i)$$
$$\times\exp(j2\pi i f_\Delta(\tau_{nm_n}(\mathbf{r}) - \tau_{nl_n}(\mathbf{r}))).$$

If the observation time is sufficiently large (as was noted above in the formulation of this problem, it must be substantially larger than correlation lengths and the maximum possible delay), we can make the following

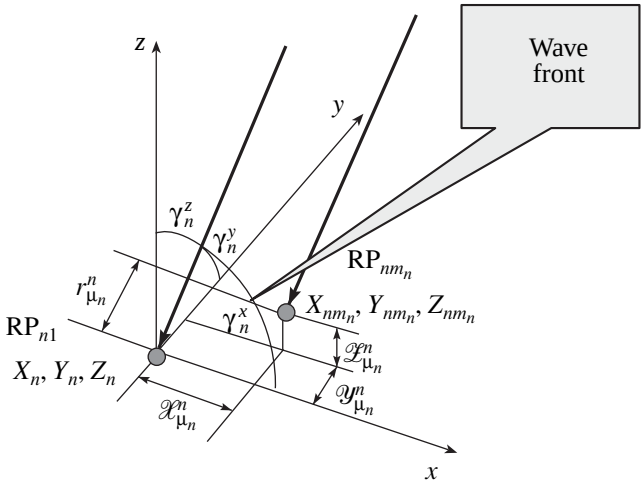

Fig. 2.

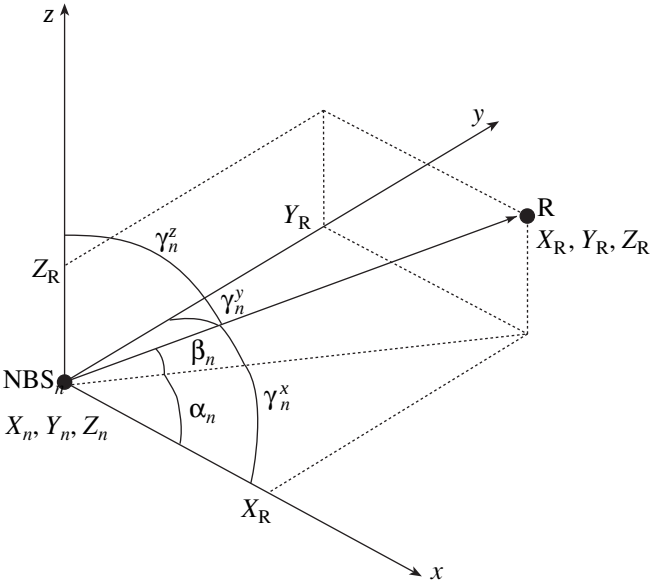

Fig. 3.

replacements: $\mathcal{U}_k(i) \longrightarrow \frac{1}{T_o} U_k(if_\Delta)$, $\mathcal{G}_{\xi nm_n}(i) \longrightarrow \frac{1}{T_o} G_{\xi nm_n}(if_\Delta)$; $\mathcal{G}_s(i) \longrightarrow \frac{1}{T_o} G_s(if_\Delta)$, $if_\Delta = f$, and $f_\Delta = \frac{1}{T_o} \longrightarrow df$. To simplify mathematical transformations, we can replace in (7) the sum over i with the sum over f.

All combinations $\tau_{nm_n}(\mathbf{r}) - \tau_{nl_n}(\mathbf{r})$ can be expressed in terms of the components of vector $\mathbf{T}_{\varphi n} = \|\tau_1^{\varphi n}(\mathbf{r}), \ldots, \tau_{M_n-1}^{\varphi n}(\mathbf{r})\|^T$, where $\tau_{\mu_n}^{\varphi n}(\mathbf{r}) = \tau_{nm_n}(\mathbf{r}) - \tau_{n1}(\mathbf{r})$, $\tau_{nm_n}(\mathbf{r}) - \tau_{nl_n}(\mathbf{r}) = \tau_{\mu_n}^{\varphi n}(\mathbf{r}) - \tau_{\lambda_n}^{\varphi n}(\mathbf{r})$, $\mu_n = m_n - 1 = \overline{1, M_n - 1}$, $\lambda_n = l_n - 1 = \overline{0, M_n - 2}$ ($\mu_n > \lambda_n$), and $\tau_0^{\varphi n}(\mathbf{r}) \equiv 0$. Vector $\mathbf{T}_{\varphi n}$ is composed of delays between the signal of the center RP in the nth NBS (here, the center RP is the first RP of the nth NBS) and remaining $M_n - 1$ signals of the nth NBS. Delays $\tau_{\mu_n}^{\varphi n}$ are comparable to $\frac{1}{f_0}$; therefore, they can be called phase delays. By f_0, we mean quantity $f_0 = (f_2 + f_1)/2$, where f_2 and f_1 are the upper and lower signal frequencies.

Taking into account that the largest distance between RPs in an NBS is substantially less than the distance to radiator, we can use the model of plane wave front (Fig. 2) and represent the nth NBS (NBS$_n$) by a point object (Fig. 3). Then, components of vector $\mathbf{T}_{\varphi n}$ can be written as $\tau_{\mu_n}^{\varphi n}(\mathbf{r}) = \frac{1}{c} r_{\mu_n}^n$, where

$$r_{\mu_n}^n = \mathcal{X}_{\mu_n}^n \cos(\gamma_n^x(\mathbf{r})) + \mathcal{Y}_{\mu_n}^n \cos(\gamma_n^y(\mathbf{r})) + \mathcal{Z}_{\mu_n}^n \cos(\gamma_n^z(\mathbf{r})),$$

$$\mathcal{X}_{\mu_n}^n = X_{nm_n} - X_n; \quad \mathcal{Y}_{\mu_n}^n = Y_{nm_n} - Y_n;$$
$$\mathcal{Z}_{\mu_n}^n = Z_{nm_n} - Z_n,$$

$$\cos(\gamma_n^x(\mathbf{r})) = (X_R - X_n)/R_n(\mathbf{r}),$$
$$\cos(\gamma_n^y(\mathbf{r})) = (Y_R - Y_n)/R_n(\mathbf{r}),$$
$$\cos(\gamma_n^z(\mathbf{r})) = (Z_R - Z_n)/R_n(\mathbf{r}),$$

$\mathbf{r}_n \equiv \mathbf{r}_{n1} = \|X_n, Y_n, Z_n\|^T$ are coordinates of the NBS$_n$; $R_n(\mathbf{r}) \equiv R_{n1}(\mathbf{r}) = \sqrt{(\mathbf{r}_n - \mathbf{r})^T(\mathbf{r}_n - \mathbf{r})}$ is the distance from the radiator to the NBS$_n$; $\gamma_n^x(\mathbf{r})$, $\gamma_n^y(\mathbf{r})$, and $\gamma_n^z(\mathbf{r})$ are angles between axes x, y, and z, respectively, and the vector connecting the NBS$_n$ and the radiator (see Fig. 3). All angles are measured between positive directions of respective vectors along the shortest path.

In NBSs, we have the following typical relationship: for f from interval f_1–f_2 and all possible values of difference $\tau_{nm_n}(\mathbf{r}) - \tau_{nl_n}(\mathbf{r})$, $2\pi(f - f_0)(\tau_{nm_n}(\mathbf{r}) - \tau_{nl_n}(\mathbf{r})) \ll 2\pi$. Therefore, this component has almost zero effect on the result of summation (integration) in the formula for J_2. In view of this fact, we can write that $2\pi f(\tau_{nm_n}(\mathbf{r}) - \tau_{nl_n}(\mathbf{r})) = 2\pi(f - f_0)(\tau_{nm_n}(\mathbf{r}) - \tau_{nl_n}(\mathbf{r})) + 2\pi f_0(\tau_{nm_n}(\mathbf{r}) -$

$\tau_{nl_n}(\mathbf{r})) \approx 2\pi f_0(\tau_{nm_n}(\mathbf{r}) - \tau_{nl_n}(\mathbf{r})) = 2\pi f_0(\tau^{\varphi n}_{\mu_n}(\mathbf{r}) - \tau^{\varphi n}_{\lambda_n}(\mathbf{r}))$. Whence it follows that

$$J_{0n} = \sum_{m_n=1}^{M_n} \int_0^{+\infty} G^{-1}_{\xi nm_n}(f) U_{nm_n}(f) U^*_{nm_n}(f) df;$$

$$J_{1n}(a_n) = \sum_{m_n=1}^{M_n} \int_0^{+\infty} W^2_{nm_n}(f) U_{nm_n}(f) U^*_{nm_n}(f) df;$$

$$J_{2n}(\mathbf{r}, a_n) = \sum_{l_n=1}^{M_n-1} \sum_{m_n=l_n+1}^{M_n} \exp(j2\pi f_0(\tau^{\varphi n}_{\mu_n}(\mathbf{r}) - \tau^{\varphi n}_{\lambda_n}(\mathbf{r}))) \times \int_0^{+\infty} W_{nm_n}(f) W_{nl_n}(f) U_{nm_n}(f) U^*_{nl_n}(f) df;$$

where $W_{nm_n}(f) = \dfrac{1}{G_{\xi nm_n}(f)} \sqrt{\dfrac{a_n G_s(f)}{1 + \sum_{l_n=1}^{M_n} q_{nl_n}(f)}}$ is the frequency characteristic of the input filter installed in the nm_nth channel, $q_{nm_n}(f) = \dfrac{a_n G_s(f)}{G_{\xi nm_n}(f)}$ is the signal-to-noise ratio in the nm_nth channel, $\mu_n = m_n - 1$; $\lambda_n = l_n - 1$, and $\tau^{\varphi n}_{\lambda_n}(\mathbf{r}) \equiv 0$ for $\lambda_n = 0$.

The real part of $J_{2n}(\mathbf{r}, a_n)$ can be written as

$$\mathrm{Re}(J_{2n}(\mathbf{r}, a_n)) = \sum_{l_n=1}^{M_n-1} \sum_{m_n=l_n+1}^{M_n} A_{nm_nnl_n} \times \cos(2\pi f_0(\tau^{\varphi n}_{\mu_n}(\mathbf{r}) - \tau^{\varphi n}_{\lambda_n}(\mathbf{r})) + \Phi_{nm_nnl_n}), \quad (8)$$

where

$$\Phi_{nm_nnl_n} = \arctan\left\{\int_0^{\infty} W_{nm_n}(f) W_{nl_n}(f) |U_{nm_n}(f)| |U_{nl_n}(f)| \times \sin(\varphi_{nm_n}(f) - \varphi_{nl_n}(f)) df, \int_0^{\infty} W_{nm_n}(f) W_{nl_n}(f) \times |U_{nm_n}(f)| |U_{nl_n}(f)| \cos(\varphi_{nm_n}(f) - \varphi_{nl_n}(f)) df \right\}$$

is the difference of "pseudophases" for signals of the m_nth and l_nth reception points in the nth NBS,

$$A_{nm_nnl_n} = \left\{\left[\int_0^{\infty} W_{nm_n}(f) W_{nl_n}(f) |U_{nm_n}(f)| |U_{nl_n}(f)| \times \sin(\varphi_{nm_n}(f) - \varphi_{nl_n}(f)) df\right]^2 + \left[\int_0^{\infty} W_{nm_n}(f) W_{nl_n}(f) \times |U_{nm_n}(f)| |U_{nl_n}(f)| \cos(\varphi_{nm_n}(f) - \varphi_{nl_n}(f)) df\right]^2\right\}^{1/2}$$

is the total "pseudoamplitude," $\varphi_{nm_n}(f) = \arctan\{\mathrm{Im}(U_{nm_n}(f)), \mathrm{Re}(U_{nm_n}(f))\}$ is the phase-response characteristic of the signal received at the m_nth reception point of the nth NBS, $\arctan(b, c) = \arctan(b/c)$ for $c > 0$, $\arctan(b, c) = \arctan(b/c) + \mathrm{sgn}(b)\dfrac{\pi}{2}$ for $c < 0$, $\mathrm{sgn}(b) = 1(-1)$ for $b > 0$ ($b < 0$), $\arctan(b, 0) = \mathrm{sgn}(b)\dfrac{\pi}{2}$ for $b \neq 0$, and $\arctan(0, 0) = 0$.

In order to calculate normalizing factor $C_n(\mathbf{a})$, we should find the determinant of matrix $\mathbf{G}(\mathbf{r}, \mathbf{a})$. Using the definition of matrix $\mathbf{G}(\mathbf{r}, \mathbf{a})$ given in (4), we can write

$$|\mathbf{G}(\mathbf{r}, \mathbf{a})| = \prod_{n=1}^{N} \prod_{i=0}^{I-1} |\mathbf{G}_n(i)|. \quad (9)$$

In order to find $|\mathbf{G}_n(i)|$, we should take into account the following formula valid for determinants of square matrices $\mathbf{A}$ and $\mathbf{B}$ of the same order: $|\mathbf{AB}| = |\mathbf{BA}| = |\mathbf{A}||\mathbf{B}|$ [3, Section 13.2]. Moreover, for $N \times N$ matrix $\mathbf{Z} = \mathbf{1} + \mathbf{X}$, where $\mathbf{X}$ is the diagonal matrix with elements $X_1, \ldots, X_N$, we have $|\mathbf{Z}| = (\prod_1^N X_n)(1 + 1/X_1 + 1/X_2 + \ldots + 1/X_N)$. Using this fact, we can write

$$|\mathbf{G}_n(i)| = \left(\prod_{m_n=1}^{M_n} \mathcal{G}_{\xi nm_n}(i)\right)\left(1 + \sum_{m_n=1}^{M_n} a_n \frac{\mathcal{G}_s(i)}{\mathcal{G}_{\xi nm_n}(i)}\right); \quad (10)$$

$$C_n(\mathbf{a}) = (2\pi)^{-I\mathcal{M}/2} \times \left\{\prod_{n=1}^{N} \prod_{i=0}^{I-1} \left[\left(\prod_{m_n=1}^{M_n} \mathcal{G}_{\xi nm_n}(i)\right)\left(1 + \sum_{m_n=1}^{M_n} a_n \frac{\mathcal{G}_s(i)}{\mathcal{G}_{\xi nm_n}(i)}\right)\right]\right\}^{-1/2}. \quad (11)$$

Calculating the logarithm of expression (11) and using passages to the limit preceding formula (8), we obtain

$$\ln(P(\mathbf{U}|\mathbf{r}, \mathbf{a})) = (-I\mathcal{M}/2)\ln(2\pi) - \frac{1}{2}\sum_{n=1}^{N}\left[\left(T_o \sum_{m_n=1}^{M_n} \int_0^{\infty} \ln(T_o G_{\xi nm_n}(f)) df\right) + J_{0n}\right] + L(\mathbf{r}, \mathbf{a}),$$

where

$$L(\mathbf{r}, \mathbf{a}) = \sum_{n=1}^{N} L_n(\mathbf{r}, a_n); \quad (12)$$

$$L_n(\mathbf{r}, a_n) = \frac{1}{2}(J_{1n}(a_n) - J_{3n}(a_n)) + \mathrm{Re}(J_{2n}(\mathbf{r}, a_n)); \quad (13)$$

$$J_{3n}(a_n) = T_o \int_0^{\infty} \ln\left(1 + \sum_{m_n=1}^{M_n} a_n \frac{G_s(f)}{G_{\xi n m_n}(f)}\right) df.$$

Thus, the one-stage position-finding algorithm should form maximum-likelihood estimates of radiator coordinates $\hat{\mathbf{r}}$ and amplitude factors $\hat{\mathbf{a}}$:

$$L(\hat{\mathbf{r}}, \hat{\mathbf{a}}) = \max_{\mathbf{r} \in \mathbf{R}, \mathbf{a} \in \mathbf{A}} L(\mathbf{r}, \mathbf{a}). \quad (14)$$

A possible implementation of the position-finding system operating in accordance with formulas (12)–(14) is considered below (see Section 6 and Fig. 14).

4. ACCURACY OF ESTIMATION OF THE RADIATOR POSITION

The potential accuracy of estimation of radiator coordinates $\mathbf{r}$ and vector $\mathbf{a}$ is determined by Cramér–Rao matrix bound $\mathbf{\Phi}_{\mathrm{CR}}$ equal to the matrix that is the inverse of Fisher information matrix $\mathbf{\Phi}$: $\mathbf{\Phi}_{\mathrm{CR}} = \begin{Vmatrix} \mathbf{\Phi}_{\mathrm{CR}}^{(1)} & \mathbf{\Phi}_{\mathrm{CR}}^{(2)} \\ (\mathbf{\Phi}_{\mathrm{CR}}^{(2)})^T & \mathbf{\Phi}_{\mathrm{CR}}^{(3)} \end{Vmatrix} = \mathbf{\Phi}^{-1}$, where $\mathbf{\Phi} = \begin{Vmatrix} \mathbf{\Phi}_1 & \mathbf{\Phi}_2 \\ \mathbf{\Phi}_2^T & \mathbf{\Phi}_3 \end{Vmatrix}$.

Elements of Fisher matrix $\mathbf{\Phi}$ are determined as follows:

$$\mathcal{F}_{ij}^{(1)} = -\mathrm{M}\left(\frac{\partial^2 L(\mathbf{r}, \mathbf{a})}{\partial r_i \partial r_j}\right)_{\substack{\mathbf{r}=\hat{\mathbf{r}} \\ \mathbf{a}=\hat{\mathbf{a}}}}$$

$$= -\mathrm{M}\left(\sum_{b=1}^{N} \sum_{\lambda_b=1}^{M_b-1} \sum_{\mu_b=1}^{M_b-1} \frac{\partial^2 L(\mathbf{r}, \mathbf{a})}{\partial \tau_{\lambda_b}^{\varphi b} \partial \tau_{\mu_b}^{\varphi b}} \frac{\partial \tau_{\mu_b}^{\varphi b}}{\partial r_j} \frac{\partial \tau_{\lambda_b}^{\varphi b}}{\partial r_i} + \sum_{b=1}^{N} \sum_{k_b=1}^{M_b-1} \frac{\partial L(\mathbf{r}, \mathbf{a})}{\partial \tau_{k_b}^{\varphi b}} \frac{\partial^2 \tau_{k_b}^{\varphi b}}{\partial r_i \partial r_j}\right)_{\substack{\mathbf{r}=\hat{\mathbf{r}} \\ \mathbf{a}=\hat{\mathbf{a}}}},$$

$$\mathcal{F}_{in}^{(2)} = -\mathrm{M}\left(\frac{\partial^2 L(\mathbf{r}, \mathbf{a})}{\partial r_i \partial a_n}\right)_{\substack{\mathbf{r}=\hat{\mathbf{r}} \\ \mathbf{a}=\hat{\mathbf{a}}}} = 0,$$

$$\mathcal{F}_{mn}^{(3)} = -\mathrm{M}\left(\frac{\partial^2 L(\mathbf{r}, \mathbf{a})}{\partial a_m \partial a_n}\right)_{\substack{\mathbf{r}=\hat{\mathbf{r}} \\ \mathbf{a}=\hat{\mathbf{a}}}}, \quad i, j = \overline{1, 3},$$

$$r_1 \equiv X_{\mathrm{R}}, \quad r_2 \equiv Y_{\mathrm{R}}, \quad r_3 \equiv Z_{\mathrm{R}}, \quad m, n = \overline{1, N}.$$

Differentiating expression (12) and calculating the mean value at point $(\hat{\mathbf{a}}, \hat{\mathbf{r}})$, we obtain

$$\mathrm{M}\left(\frac{\partial^2 L(\mathbf{r}, \mathbf{a})}{\partial \tau_{\lambda_b}^{\varphi b} \partial \tau_{\mu_b}^{\varphi b}}\right)_{\substack{\mathbf{r}=\hat{\mathbf{r}} \\ \mathbf{a}=\hat{\mathbf{a}}}} = \begin{cases} -\sum_{\substack{i=1 \\ i \neq m_b}}^{M_b} P_{i m_b}, & \mu_b = \lambda_b, \\ P_{m_b l_b}, & \mu_b \neq \lambda_b, \end{cases}$$

$$m_b = \mu_b + 1, \quad l_b = \lambda_b + 1, \quad \mu_b, \lambda_b = \overline{1, M_b - 1};$$

$$P_{m_b l_b} = 2T_o(2\pi f_0)^2 \times \int_0^{+\infty} q_{b m_b}(f) q_{b l_b}(f) \Big/ \left[1 + \sum_{n_b=1}^{M_b} q_{b n_b}(f)\right] df;$$

$$\mathrm{M}\left(\frac{\partial L(\mathbf{r}, \mathbf{a})}{\partial \tau_{k_b}^{\varphi b}}\right)_{\substack{\mathbf{r}=\hat{\mathbf{r}} \\ \mathbf{a}=\hat{\mathbf{a}}}} = 0;$$

$$\mathrm{M}\left(\frac{\partial^2 L(\mathbf{r}, \mathbf{a})}{\partial a_n^2}\right)_{\substack{\mathbf{r}=\hat{\mathbf{r}} \\ \mathbf{a}=\hat{\mathbf{a}}}} = \frac{1}{2} T_o \sum_{n=1}^{N} \int_0^{\infty} \left(\sum_{m_n=1}^{M_n} \frac{G_s(f)}{G_{\xi n m_n}(f)}\right)^2 \times \left(1 + \sum_{m_n=1}^{M_n} a_n \frac{G_s(f)}{G_{\xi n m_n}(f)}\right)^{-2} df$$

$$- T_o \sum_{n=1}^{N} \sum_{m_n=1}^{M_n} \int_0^{+\infty} \frac{G_s(f)(a_n G_s(f) + G_{\xi n m_n}(f))}{G_{\xi n m_n}^2(f)} \times \left(\sum_{m_n=1}^{M_n} \frac{G_s(f)}{G_{\xi n m_n}(f)}\right)\left(1 + \sum_{m_n=1}^{M_n} a_n \frac{G_s(f)}{G_{\xi n m_n}(f)}\right)^{-3} df$$

$$- 2T_o \sum_{n=1}^{N} \sum_{l_n=1}^{M_n-1} \sum_{m_n=l_n+1}^{M_n} \int_0^{\infty} \frac{a_n G_s^2(f)}{G_{\xi n m_n}(f) G_{\xi n l_n}(f)} \times \left(\sum_{m_n=1}^{M_n} \frac{G_s(f)}{G_{\xi n m_n}(f)}\right)\left(1 + \sum_{m_n=1}^{M_n} a_n \frac{G_s(f)}{G_{\xi n m_n}(f)}\right)^{-3} df;$$

$$\mathrm{M}\left(\frac{\partial^2 L(\mathbf{r}, \mathbf{a})}{\partial a_n \partial a_m}\right)_{\substack{\mathbf{r}=\hat{\mathbf{r}} \\ \mathbf{a}=\hat{\mathbf{a}}}} = 0, \quad n \neq m.$$

Thus, $\mathbf{\Phi}_{\mathrm{CR}}^{(2)}$ and, consequently, $\mathbf{\Phi}_2$ are zero matrices. As a result, $\mathbf{\Phi}_1 = (\mathbf{\Phi}_{\mathrm{CR}}^{(1)})^{-1}$ and $\mathbf{\Phi}_3 = (\mathbf{\Phi}_{\mathrm{CR}}^{(3)})^{-1}$.

Matrix $\mathbf{\Phi}_1$ can be written as

$$\mathbf{\Phi}_1 = \sum_{n=1}^{N} \mathbf{B}_n^T \mathbf{\Phi}_{\mathbf{T}_{\varphi n}}^{-1} \mathbf{B}_n, \quad (15)$$

where matrix $\mathbf{B}_n$ consists of elements

$$B_n(\mu_n, 1) = \frac{\partial\tau^{\varphi n}_{\mu_n}}{\partial r_1} \equiv \frac{\partial\tau^{\varphi n}_{\mu_n}}{\partial X_{\mathrm{R}}}$$

$$= \frac{1}{c}[\mathscr{X}^n_{\mu_n} - r^n_{\mu_n}\cos(\gamma^x_n(\mathbf{r}))]/R_n(\mathbf{r});$$

$$B_n(\mu_n, 2) = \frac{\partial\tau^{\varphi n}_{\mu_n}}{\partial r_2} \equiv \frac{\partial\tau^{\varphi n}_{\mu_n}}{\partial Y_{\mathrm{R}}}$$

$$= \frac{1}{c}[\mathscr{Y}^n_{\mu_n} - r^n_{\mu_n}\cos(\gamma^y_n(\mathbf{r}))]/R_n(\mathbf{r});$$

$$B_n(\mu_n, 3) = \frac{\partial\tau^{\varphi n}_{\mu_n}}{\partial r_3} \equiv \frac{\partial\tau^{\varphi n}_{\mu_n}}{\partial Z_{\mathrm{R}}}$$

$$= \frac{1}{c}[\mathscr{Z}^n_{\mu_n} - r^n_{\mu_n}\cos(\gamma^z_n(\mathbf{r}))]/R_n(\mathbf{r}); \quad \mu_n = \overline{1, M_n - 1},$$

and matrix $\mathbf{\Phi}^{-1}_{\mathbf{T}_{\varphi n}}$ contains elements $\Phi^{-1}_{\mathbf{T}_{\varphi n}}(\mu_n, l_n) = -\mathrm{M}\left(\frac{\partial^2 L(\mathbf{r}, \mathbf{a})}{\partial\tau^{\varphi n}_{\lambda_n}\partial\tau^{\varphi n}_{\mu_n}}\right)$, $\lambda_n, \mu_n = \overline{1, M_n - 1}$.

Hence, the potential accuracy of coordinate estimation for the one-stage method is described by the matrix

$$\mathbf{\Phi}_{\mathrm{os}} = \mathbf{\Phi}^{(1)}_{\mathrm{CR}} = (\mathbf{\Phi}_1)^{-1}. \tag{16}$$

The structure of matrix $\mathbf{\Phi}_{\mathbf{T}_{\varphi n}}$, which is the inverse matrix for matrix $\mathbf{\Phi}^{-1}_{\mathbf{T}_{\varphi n}}$ appearing in (15), is also of interest. The reason is that the phase-comparison direction-finding systems use, as a rule, a two-stage bearing measurement procedure. The first stage lies in measuring phase delays that are recalculated to bearing angles at the second stage (see, for example, [4]).

Let us consider the structure of matrix $\mathbf{\Phi}_{\mathbf{T}_{\varphi n}}$ for the case when signal-to-noise ratios are the same for all RPs and are uniform within frequency band $2\Delta_f = f_2 - f_1$. In this case, $q_{nm_n}(f) = q_{kl_k}(f) = q$; consequently, $P_{m_b l_b} = P_{n_k j_k} = P$, $a_n = a_m = a$, and $G_{\xi nm_n}(f) = \mathscr{G}_{\xi kl_k}(f) = \mathscr{G}_\xi$. In addition, we assume that the number of RPs is the same for all NBSs, i.e., $M_n = M_k = M$. Then,

$$\mathbf{\Phi}^{-1}_{\mathbf{T}_{\varphi n}} = P(M\mathbf{E} - \mathbf{1}), \tag{17}$$

where $P = 16\pi^2 T_{\mathrm{o}} f_0^2 \Delta_f q^2/(1 + Mq)$, matrices $\mathbf{E}$ and $\mathbf{1}$ have dimensions $(M-1)\times(M-1)$, and

$$\mathbf{\Phi}_{\mathbf{T}_{\varphi n}} = \frac{1}{PM}(\mathbf{E} + \mathbf{1}). \tag{18}$$

Diagonal elements of matrix $\mathbf{\Phi}_{\mathbf{T}_{\varphi n}}$ can be represented as $\sigma^2_{\tau_\varphi} = \frac{2}{PM}$. In this case,

$$\sigma^2_{\tau_\varphi} = \frac{1 + Mq}{8\pi^2 T_{\mathrm{o}} f_0^2 \Delta_f M q^2}. \tag{19}$$

In expression (14), we estimate not only informative parameter $\mathbf{r}$ but also noninformative parameter $\mathbf{a}$. Implementing rule (14), we have a vexed problem of the first approximation to amplitude vector $\mathbf{a}$, because we know nothing about its distribution law. Below, we propose a heuristic method enabling formation of the preliminary estimate of vector $\mathbf{a}$. The potential measurement accuracy for vector $\mathbf{a}$ is described by matrix $\mathbf{\Phi}^{(3)}_{\mathrm{CR}}$, which is the inverse matrix for matrix $\mathbf{\Phi}_3$.

Matrices $\mathbf{\Phi}^{(3)}_{\mathrm{CR}}$ and $\mathbf{\Phi}_3$ are diagonal. Taking into account the above assumptions, we can write

$$\mathbf{\Phi}^{(3)}_{\mathrm{CR}} = \sigma_a^2 \mathbf{E}_N, \tag{20}$$

where $\mathbf{E}_N$ is the $N\times N$ identity matrix and σ_a^2 is the variance of the measurement error for amplitude factor a. The relative error is

$$\frac{\sigma_a}{a} = \frac{Mq + 1}{Mq\sqrt{T_{\mathrm{o}} 2\Delta_f N}}. \tag{21}$$

5. COMPARATIVE ANALYSIS OF ONE-STAGE AND DIRECTION-FINDING METHODS FOR DETERMINING THE RADIATOR POSITION

Let us consider the procedure for measuring the radiator coordinates with an intermediate stage (measurement of bearing angles). Below, we call this procedure the direction-finding algorithm. In this algorithm, the nth NBS determines estimates of azimuth and elevation angles $\hat{\alpha}_n$ and $\hat{\beta}_n$ (Fig. 4) and signal amplitudes $\hat{a}_n$ according to the rule

$$\mathscr{L}_n(\hat{\alpha}_n, \hat{\beta}_n, \hat{a}_n) = \max_{\alpha_n \in \mathbf{A}, \beta_n \in \mathbf{B}, a_n \in \mathfrak{A}} \mathscr{L}_n(\alpha_n, \beta_n, a_n), \tag{22}$$

where

$$\mathscr{L}_n(\alpha_n, \beta_n, a_n) = \frac{1}{2}(J_{1n}(a_n) - J_{3n}(a_n)) + \mathrm{Re}(\mathscr{J}_{2n}(\alpha_n, \beta_n, a_n))]\}; \tag{23}$$

designations $J_{1n}(a_n)$ and $J_{3n}(a_n)$ were explained in com-

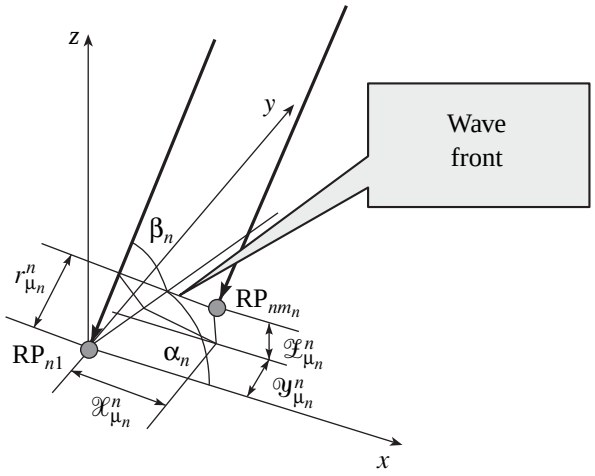

Fig. 4.

ments to expressions (8) and (13), respectively; and

$$\mathrm{Re}(\mathcal{J}_{2n}(\alpha_n, \beta_n, a_n)) = \sum_{l_n=1}^{M_n-1} \sum_{m_n=l_n+1}^{M_n} A_{nm_nnl_n} \times \cos(2\pi f_0(\tau^{\varphi n}_{\mu_n}(\alpha_n, \beta_n) - \tau^{\varphi n}_{\lambda_n}(\alpha_n, \beta_n)) + \Phi_{nm_nnl_n}); \quad (24)$$

$$\mu_n = m_n - 1,\ \lambda_n = l_n - 1,\ \tau^{\varphi n}_{\lambda_n}(\mathbf{r}) \equiv 0 \text{ for } \lambda_n = 0.$$

All components of expressions (22)–(24) were already determined above except for $\tau^{\varphi n}_{\mu_n}(\alpha_n, \beta_n)$ (where $\mu_n = \overline{1, M_n - 1}$). In this case, $\tau^{\varphi n}_{\mu_n}(\alpha_n, \beta_n) = (1/c) r^n_{\mu_n}$, where

$$r^n_{\mu_n} = \mathcal{X}^n_{\mu_n}\cos(\alpha_n)\cos(\beta_n) + \mathcal{Y}^n_{\mu_n}\sin(\alpha_n)\cos(\beta_n) + \mathcal{Z}^n_{\mu_n}\sin(\beta_n).$$

The matrix describing the potential accuracy of measuring azimuth and elevation angles in the nth NBS is similar to that appearing in formula (15):

$$\mathfrak{F}_n = \begin{Vmatrix} \sigma^2_{n\alpha} & \sigma^2_{n\alpha\beta} \\ \sigma^2_{n\alpha\beta} & \sigma^2_{n\beta} \end{Vmatrix} = (\mathfrak{B}_n^T \mathbf{\Phi}^{-1}_{\mathbf{T}_{\varphi n}} \mathfrak{B}_n)^{-1}, \quad (25)$$

where elements of matrix $\mathfrak{B}_n$ are given by

$$B_n(\mu_n, 1) = \frac{\partial \tau^{\varphi n}_{\mu_n}}{\partial \alpha_n} = \frac{1}{c}[-\mathcal{X}^n_{\mu_n}\sin(\alpha_n)\cos(\beta_n) + \mathcal{Y}^n_{\mu_n}\cos(\alpha_n)\cos(\beta_n)],$$

$$B_n(\mu_n, 2) = \frac{\partial \tau^{\varphi n}_{\mu_n}}{\partial \beta_n} = \frac{1}{c}[-\mathcal{X}^n_{\mu_n}\cos(\alpha_n)\sin(\beta_n) - \mathcal{Y}^n_{\mu_n}\sin(\alpha_n)\sin(\beta_n) + \mathcal{Z}^n_{\mu_n}\sin(\beta_n)].$$

In the direction-finding method, the radiator coordinates are estimated according to the rule [5, expression (12)]

$$\hat{\mathbf{r}} = \mathbf{r}_0 + (\mathfrak{B}_\mathbf{r}^T \mathfrak{F}^{-1} \mathfrak{B}_\mathbf{r})^{-1} \mathfrak{B}_\mathbf{r}^T \mathfrak{F}^{-1}(\hat{\boldsymbol{\theta}} - \boldsymbol{\theta}(\mathbf{r}_0)). \quad (26)$$

Here, $\boldsymbol{\theta} = \|\alpha_1, \beta_1, \ldots, \alpha_N, \beta_N\|$; $\mathfrak{F} = \mathrm{diag}(\mathfrak{F}_n)$ is the $2N \times 2N$ matrix consisting of $N \times N$ submatrices of which nonzero ones only (n,n)th 2×2 submatrices $\mathfrak{F}_n$ situated on the diagonal,

$$\mathfrak{B}_\mathbf{r} = \left\| \mathfrak{B}^T_{\mathbf{r}1}, \ldots, \mathfrak{B}^T_{\mathbf{r}N} \right\|^T; \quad \mathfrak{B}_{\mathbf{r}n} = \begin{Vmatrix} \frac{\partial \alpha_n}{\partial X_\mathrm{R}} & \frac{\partial \alpha_n}{\partial Y_\mathrm{R}} & \frac{\partial \alpha_n}{\partial Z_\mathrm{R}} \\ \frac{\partial \beta_n}{\partial X_\mathrm{R}} & \frac{\partial \beta_n}{\partial Y_\mathrm{R}} & \frac{\partial \beta_n}{\partial Z_\mathrm{R}} \end{Vmatrix},$$

$$n = \overline{1, N};$$

and vector $\mathbf{r}_0$ denotes coordinates of the reference point.

As follows from Fig. 3,

$$\alpha_n = \arctan\{(Y_\mathrm{R} - Y_n)/(X_\mathrm{R} - X_n)\},$$

$$\beta_n = \arcsin\{(Z_\mathrm{R} - Z_n)/[(X_\mathrm{R} - X_n)^2 + (Y_\mathrm{R} - Y_n)^2 + (Z_\mathrm{R} - Z_n)^2]^{1/2}\}.$$

Thus,

$$\frac{\partial \alpha_n}{\partial X_\mathrm{R}} = -\sin(\alpha_n)/\mathcal{R}_n; \quad \frac{\partial \alpha_n}{\partial Y_\mathrm{R}} = \cos(\alpha_n)/\mathcal{R}_n;$$

$$\frac{\partial \alpha_n}{\partial Z_\mathrm{R}} = 0; \quad \frac{\partial \beta_n}{\partial X_\mathrm{R}} = -\sin(\beta_n)\cos(\alpha_n)/R_n;$$

$$\frac{\partial \beta_n}{\partial Y_\mathrm{R}} = -\sin(\beta_n)\sin(\alpha_n)/R_n; \quad \frac{\partial \beta_n}{\partial Z_\mathrm{R}} = \cos(\beta_n)/R_n,$$

where

$$\mathcal{R}_n = [(X_\mathrm{R} - X_n)^2 + (Y_\mathrm{R} - Y_n)^2]^{1/2};$$

$$R_n = [(X_\mathrm{R} - X_n)^2 + (Y_\mathrm{R} - Y_n)^2 + (Z_\mathrm{R} - Z_n)^2]^{1/2}.$$

The accuracy of coordinates estimated with the direction-finding method is determined by the formula [5, expression (16)]

$$\mathbf{\Phi}_\mathrm{df} = (\mathfrak{B}_\mathbf{r}^T \mathfrak{F}^{-1} \mathfrak{B}_\mathbf{r})^{-1}, \quad (27)$$

where $\mathfrak{F}^{-1} = \mathrm{diag}(\mathfrak{F}_n^{-1})$. Whence it follows that

$$\mathbf{\Phi}_\mathrm{df} = \left(\sum_{n=1}^{N} \mathfrak{B}^T_{\mathbf{r}n} \mathfrak{B}_n^T \mathbf{\Phi}^{-1}_{\mathbf{T}_{\varphi n}} \mathfrak{B}_n \mathfrak{B}_{\mathbf{r}n} \right)^{-1}.$$

Since $\mathfrak{B}_n \mathfrak{B}_{\mathbf{r}n} = \mathbf{B}_n$, we find that

$$\mathbf{\Phi}_\mathrm{df} = \left(\sum_{n=1}^{N} \mathbf{B}_n^T \mathbf{\Phi}^{-1}_{\mathbf{T}_{\varphi n}} \mathbf{B}_n \right)^{-1} = \mathbf{\Phi}_\mathrm{os}. \quad (28)$$

Thus, for large signal-to-noise ratios, when measurement errors are described by the Cramér–Rao bound, accuracies of the radiator coordinates estimated using the one-stage and two-stage (direction-finding) methods are identical.

6. ANALYSIS OF POSITION-FINDING ALGORITHMS IN THE PRESENCE OF ABNORMAL MEASUREMENT ERRORS

The main differences between accuracies of the radiator coordinates estimated with the one-stage and two-stage methods arise when the signal level falls below some threshold characterized by the appearance of abnormal measurement errors. To demonstrate the influence of this effect, we consider the structure of the direction-finding device shown in Fig. 5. In this case, we use the following simplifications. The narrow-base subsystem contains four RPs, each comprising an antenna with circular pattern in the azimuth plane and an RS. Using formula (25), we can readily demonstrate the well-known result (see, for example, [6, p. 221]): the accuracy of measuring the azimuth and elevation angles is directly proportional to the distance between extreme antennas. At the same time, this configuration should satisfy the condition $d < \lambda/2$, where $\lambda = c/f_0$ is the wavelength of the received signal. We will use the relationship $2d = 0.8\lambda$. In addition, we assume that the direction-finding device and the radiator are situated in the same plane.

We choose the situation in which $N = 1$. It corresponds to the case when the system measures a single bearing of the radiator or performs the first estimation of the position line in the flyby position-finding method. Then, $Z_{nm_n} = 0$ ($m_n = \overline{1, 4}$ and $n = 1$) and $Z_R = 0$. Assume that spectral densities of the signal and noise

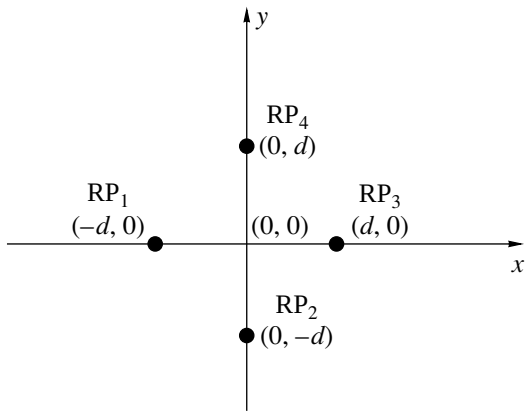

Fig. 5.

powers are the same for all RPs and are uniform in the frequency band $2\Delta_f = f_2 - f_1$. In this case, $G_{\xi nm_n}(f) = G_{\xi kl_k}(f) = G_\xi$, $G_s(f) = G_s$, and $q_{nm_n}(f) = q_{kl_k}(f) = q$ ($q = aG_s/G_\xi$). As a result, expression (23) takes the form (index n is omitted)

$$\mathcal{L}(\alpha, a) = 0.5\left\{(q^{-1} + 4)^{-1} G_\xi^{-1} \sum_{m=1}^{4} \int_{f_1}^{f_2} U_m(f) U_m^*(f) df - 2T_0 \Delta_f \ln(1 + 4q)\right\} + (q^{-1} + 4)^{-1} G_\xi^{-1} L_1(\alpha), \tag{29}$$

where

$$\mathcal{L}_1(\alpha) = \sum_{l=1}^{3} \sum_{m=l+1}^{4} \left\{\left[\int_{f_1}^{f_2} |U_m(f)||U_l(f)| \sin(\varphi_m(f) - \varphi_l(f)) df\right]^2 + \left[\int_{f_1}^{f_2} |U_m(f)||U_l(f)| \cos(\varphi_m(f) - \varphi_l(f)) df\right]^2\right\}$$

$$\times \cos\left(2\pi \frac{f_0}{c}((X_m - X_l)\cos(\alpha) + (Y_m - Y_l)\sin(\alpha)) + \Phi_{ml}\right),$$

and

$$\Phi_{ml} = \arctan\left\{\int_{f_1}^{f_2} |U_m(f)||U_l(f)| \sin(\varphi_m(f) - \varphi_l(f)) df, \int_{f_1}^{f_2} |U_m(f)||U_l(f)| \cos(\varphi_m(f) - \varphi_l(f)) df\right\}$$

is the difference of pseudophases for signals at the mth and lth RPs.

The estimate of azimuth α can be obtained in an explicit form if we retain in (29) only two terms corre-

sponding to two orthogonal pairs: RP_1–RP_3 ($l = 1$ and $m = 3$) and RP_2–RP_4 ($l = 2$ and $m = 4$). Then,

$$\hat{\alpha}_1 = \arctan(\Phi_{24}, \Phi_{13}). \quad (30)$$

Here, we took into account that $\Phi_{24} = -\Phi_{42}$ and $\Phi_{13} = -\Phi_{31}$.

The derived expression is of interest because it allows a rather simple way for finding the radiator bearing. The optimal (maximum likelihood) estimate can be found using a more complicated method:

$$\mathcal{L}_1(\hat{\alpha}) = \max_{\alpha \in \mathbf{A}} \mathcal{L}_1(\alpha). \quad (31)$$

Below, we analyze operation of heuristic (30) and optimal (31) bearing measurement algorithms using simulation on a personal computer.

The signal level is estimated using the rule

$$\mathcal{L}_2(\hat{a}) = \max_{a \in \mathbf{A}} \mathcal{L}_2(a), \quad (32)$$

where

$$\mathcal{L}_2(a) = 0.5\left\{(q^{-1} + 4)^{-1} G_\xi^{-1} \sum_{m=1}^{4} \int_{f_1}^{f_2} U_m(f) U_m^*(f) df - 2T_o \Delta_f \ln(1 + 4q)\right\} + (q^{-1} + 4)^{-1} G_\xi^{-1} \mathcal{L}_1(\hat{\alpha}).$$

Calculating the derivative of quantity $\mathcal{L}_2(a)$, taking into account that $q = aG_s/G_\xi$, and equating the result to zero, we obtain an explicit expression for the estimate of the signal amplitude (a):

$$\hat{a} = \frac{1}{4}\left\{\left[\frac{1}{4}\sum_{m=1}^{4}\int_{f_1}^{f_2} U_m(f) U_m^*(f) df + 2\mathcal{L}_1(\hat{\alpha})\right]/(2T_o\Delta_f) - G_\xi\right\}/G_s. \quad (33)$$

Estimates obtained from formulas (31) and (32) are optimal estimates only for a single measurement ($N = 1$). When we measure coordinates (i.e., when $N > 1$), these results can only be treated as auxiliary results allowing us to simplify implementation of one-stage algorithm (14), in which we should estimate not only coordinate vector **r** but also noninformative parameter **a**. Using expression (33), we can obtain a rather exact approximation to a_n ($n = \overline{1, N}$). Simulation revealed that, implementing algorithm (14), one has no need for additional refinement of the first approximation obtained from formula (33).

Let us now obtain the particular form of expression (25) for the case under study. We should take into account that $\mathfrak{B}_n = -\frac{d}{c}\|\sin(\alpha) + \cos(\alpha),\ 2\sin(\alpha),\ \sin(\alpha) - \cos(\alpha)\|^T$, $\mathbf{\Phi}_{\mathbf{T}_{\varphi n}}^{-1} = P(4\mathbf{E} - \mathbf{1})$, and $P = 16\pi^2 T_o f_0^2 \Delta_f q^2/(1 + 4q)$. Then,

$$\mathfrak{F}_n = \sigma_\alpha^2 = \left[\frac{d^2}{c^2} P(4\mathfrak{B}_n^T\mathfrak{B}_n - \mathfrak{B}_n^T \mathbf{1} \mathfrak{B}_n)\right]^{-1} = \frac{(1 + 4q)c^2}{128\pi^2 T_o f_0^2 \Delta_f q^2 d^2}. \quad (34)$$

Note that variance σ_α^2 is independent of α. Hence, for the antenna system whose configuration is shown in Fig. 5, the potential value of the bearing measurement accuracy is independent of the direction of arrival of the received signal.

Figure 6 depicts the bearing measurement error (σ_α) as a function of the signal-to-noise ratio (q). Curve *1* is the theoretical potential error calculated from formula (34); curves *2* and *3* are bearing measurement errors obtained using the personal-computer simulation of measurements carried out according to rules (31) and (30), respectively. Initial data for calculations were the following: $f_0 = 100$ MHz (accordingly, $\lambda = 1.5$ m); $d = 0.6$ m; $2\Delta_f = 32$ kHz; $T_o = 1$ ms; and $G_s = G_\xi = 1$ pW/Hz. The variance of the measured radiator bearing was estimated using the rule $\mathrm{var}_\alpha = \frac{1}{\mathcal{N} - 1}\sum_{n=1}^{\mathcal{N}} (\hat{\alpha}_n - \alpha_t)^2$, where $\mathcal{N}$ is the number of measurements (tests) and α_t is the true bearing angle.

Note that the primary goal of this simulation is to additionally check the validity of approximations and assumptions made in the course of derivation of expression (34) describing the potential measurement accuracy for a single bearing as well as to carry out the comparative analysis of explicit form (30) of the bearing estimation algorithm and optimal algorithm (31). Simulation results obtained for $q < 0$ are no longer described by bound (34); they have only qualitative character because, in this domain, the so-called abnormal measurement errors begin to play their role.

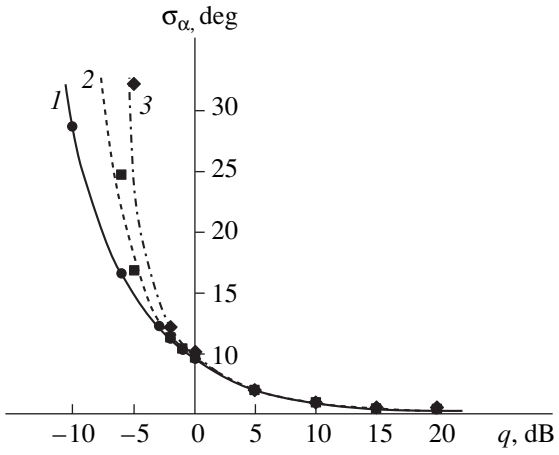

Fig. 6.

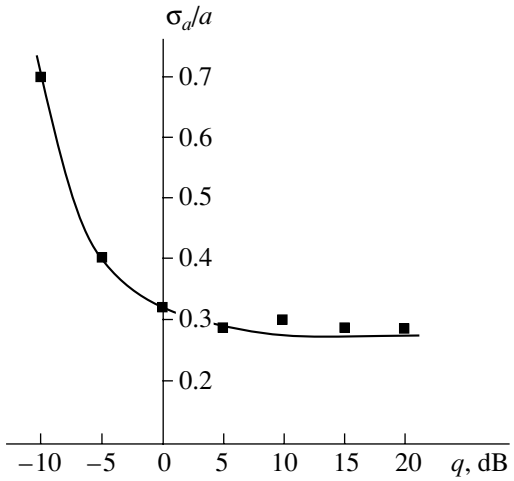

Fig. 7.

Increasing the number of measurements in this domain, we cannot obtain more stable results. Moreover, in the presence of abnormal errors, sample variance var_α no longer carries information on the quality of operation of a particular algorithm. A more objective picture can be obtained if the calculation of variance var_α is replaced with the calculation of the probability of abnormal measurement error.

As was mentioned above, the estimated amplitude obtained from rule (33) is a good initial approximation of components of vector **a** when we seek the maximum of LF (12). Let us find the excess in the potential accuracy of the measured amplitude over the accuracy of measurements carried out in accordance with formula (33). Figure 7 presents ratio $\frac{\sigma_a}{a}$ calculated as a function of signal-to-noise ratio q. The solid line corresponds to the theoretical error calculated using formula (21) and points mark relative errors of the amplitude estimated according to rule (33). The results were obtained using the numerical simulation on a personal computer. As is seen from the plot, errors in the estimated signal level are described well by the Cramér–Rao bound, including the case of small signal-to-noise ratios.

The purpose of these simulations is to additionally check the validity of assumptions made in the course of derivation of expressions related to the direction-finding algorithm, to reveal the threshold for the normal operation of this algorithm, and to find possibilities of reducing the time required for seeking the LF maximum in the one-stage algorithm that may arise due to the use of the first approximation of amplitude vector **a** based on rule (33).

Let us now analyze the one-stage algorithm itself and compare its efficiency with that of the direction-finding algorithm. In order to measure coordinates, we should fulfill the condition $N > 1$. In this case, potential accuracies of coordinate measurements performed using the one-stage and direction-finding algorithms are identical. Their values can be determined as follows:

$$\mathbf{\Phi}_{\mathrm{os}} = \mathbf{\Phi}_{\mathrm{df}} = \begin{Vmatrix} \sigma_x^2 & \sigma_{xy}^2 \\ \sigma_{xy}^2 & \sigma_y^2 \end{Vmatrix} = \sigma_r^2 \mathbf{B}_{rN}^{-1}, \qquad (35)$$

where

$$\mathbf{B}_{rN} = \begin{Vmatrix} B_1 & B_2 \\ B_2 & B_3 \end{Vmatrix}; \quad B_1 = \sum_{n=1}^{N} \frac{\sin^2 \alpha_n}{R_n};$$

$$B_2 = \sum_{n=1}^{N} -\frac{\sin \alpha_n \cos \alpha_n}{R_n}; \quad B_3 = \sum_{n=1}^{N} \frac{\cos^2 \alpha_n}{R_n}.$$

Let us perform a comparative analysis by simulating operation of the one-stage and direction-finding algorithms in the following system for determining the radi-

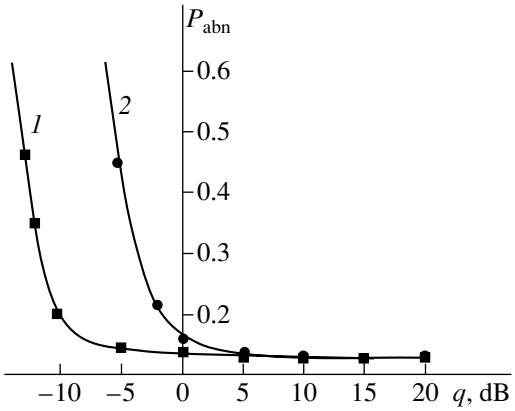

Fig. 8.

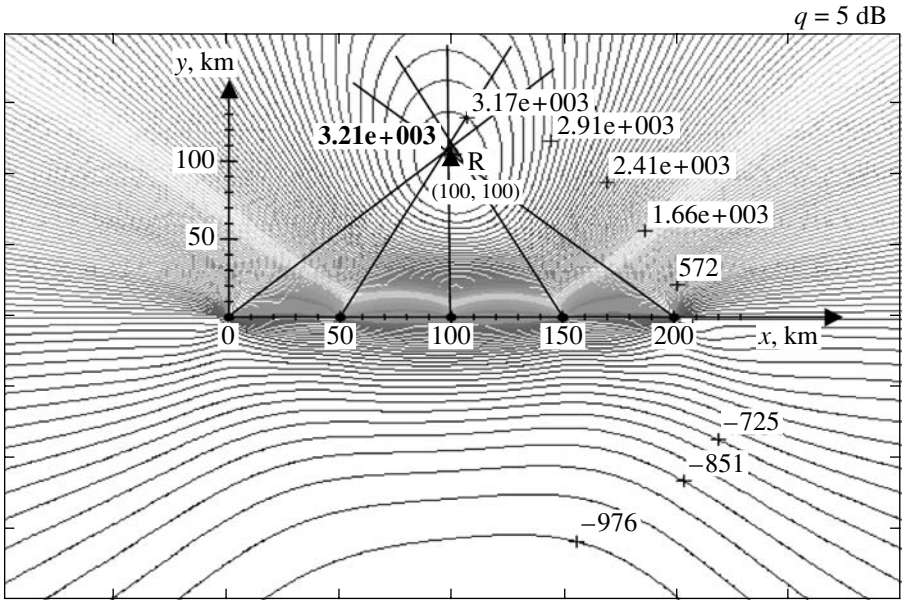

Fig. 9.

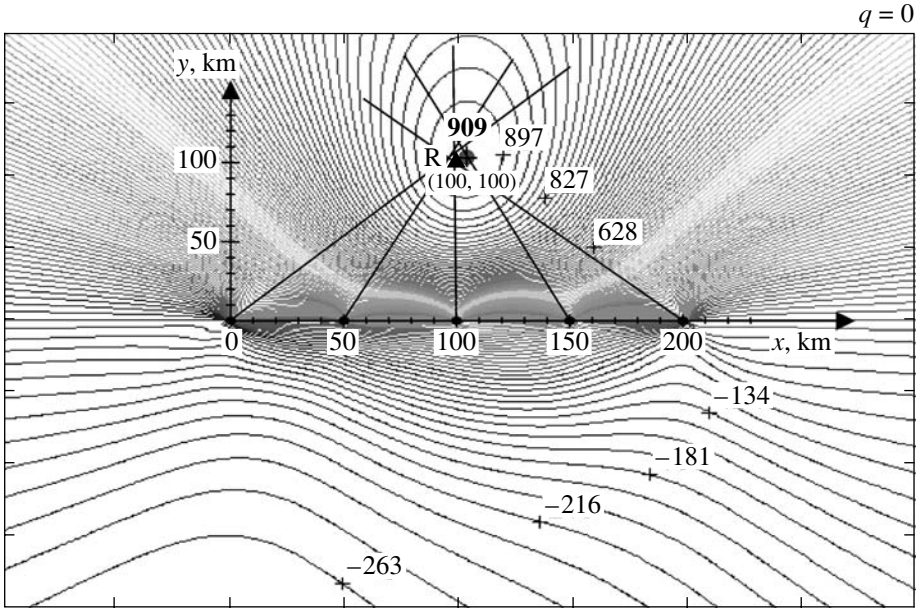

Fig. 10.

ator coordinates. Let us have a carrier moving in space for some time. An NBS whose antenna system is shown in Fig. 5 is installed onboard the carrier. We consider the coordinate determination problem for the radiator situated on a plane. If the carrier is an aircraft, the distance from the radiator to the carrier is assumed to be substantially larger than the flight altitude (i.e., the flight altitude is neglected). Positions at which the measurements are carried out are marked by points on the 0*x* axes in Figs. 9–13.

The initial parameters were the following: the radiator coordinates are X_R = 100 km and Y_R = 100 km; coordinates of five sites at which the measurements were carried out (in kilometers) are $\mathbf{r} = \|\mathbf{r}_1^T, \ldots, \mathbf{r}_5^T\| = \|0.0, 50.0, 100.0, 150.0, 200.0\|$; the area containing the radiator is 400×400 km; the center signal frequency is 100 MHz; the intermediate frequency is chosen below the halved signal sampling frequency and equals 20 MHz; the number of time-domain samples is

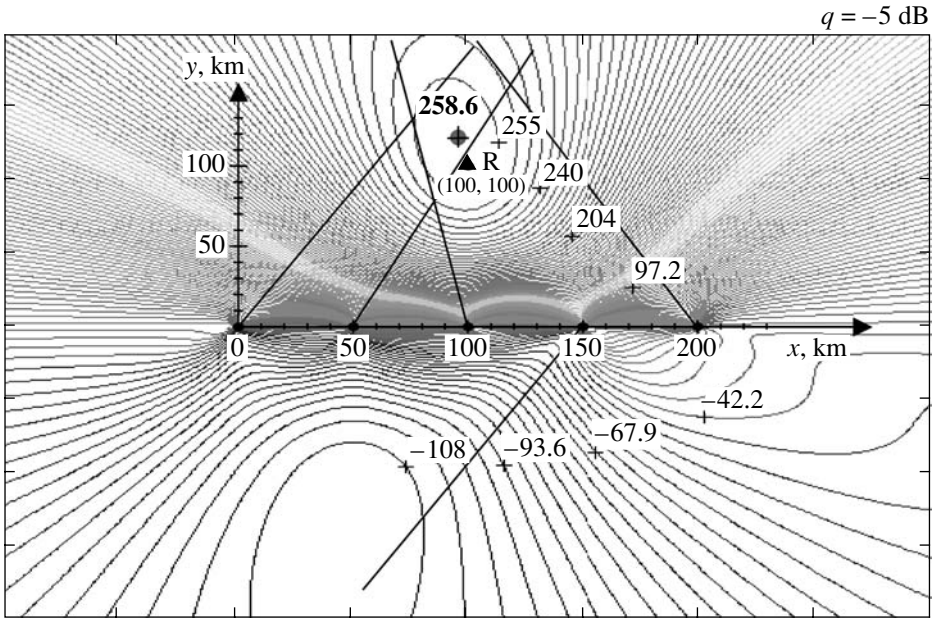

Fig. 11.

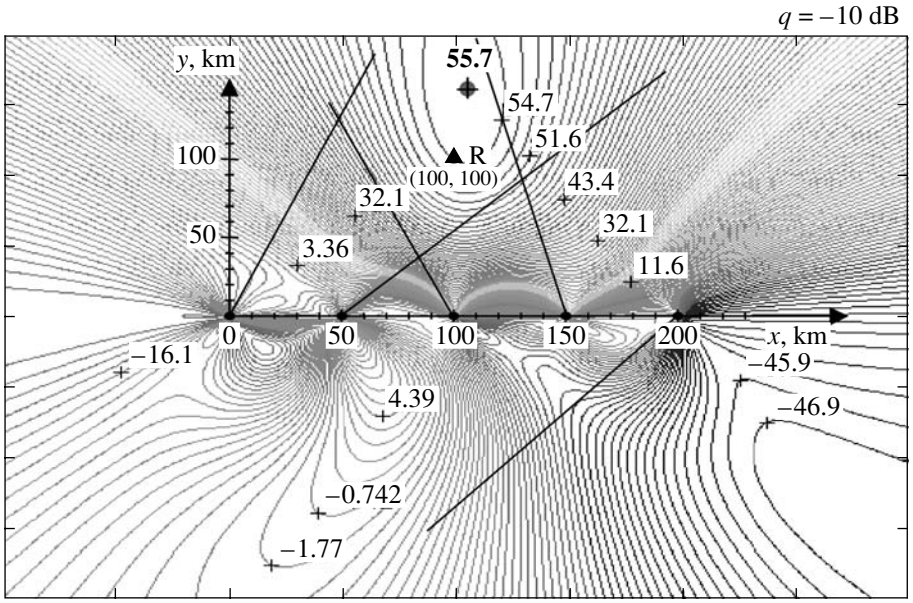

Fig. 12.

131072 within observation interval T_o = 1 ms; the signal sampling frequency is 131072 kHz; and signal bandwidth is 32 kHz.

Qualities of operation of the one-stage and direction-finding algorithms are compared using probabilities of abnormal estimation of the radiator coordinates, for which we use the probability that absolute value of error $\sqrt{\Delta_x^2 + \Delta_y^2}$ ($\Delta_x = \hat{X} - X_R$ and $\Delta_y = \hat{Y} - Y_R$, where $\hat{X}$ and $\hat{Y}$ and X_R and Y_R are measured and true radiator's coordinates, respectively) exceeds $3\sqrt{\sigma_x^2 + \sigma_y^2}$, where σ_x^2 and σ_y^2 are diagonal elements of matrix $\mathbf{\Phi}_{os}$ in formula (35).

Figure 8 depicts probability of abnormal estimate P_{abn} as a function of signal-to-noise ratio q for the one-stage (curve *1*) and two-stage (curve *2*) algorithms. One can see that, for the chosen conditions and small values of the signal-to-noise ratio, the synthesized one-stage algorithm offers an advantage over the two-stage (direction-finding) one by about 6–8 dB.

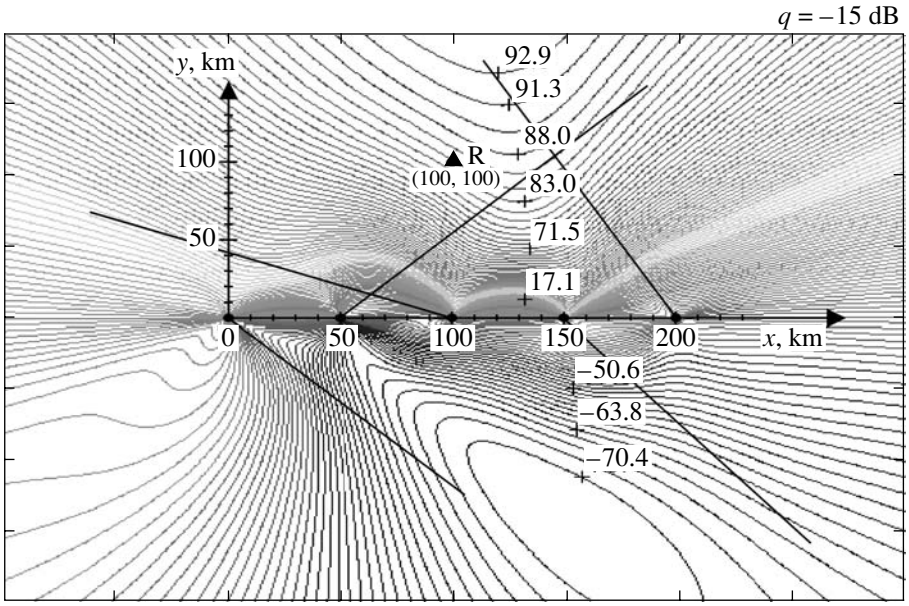

Fig. 13.

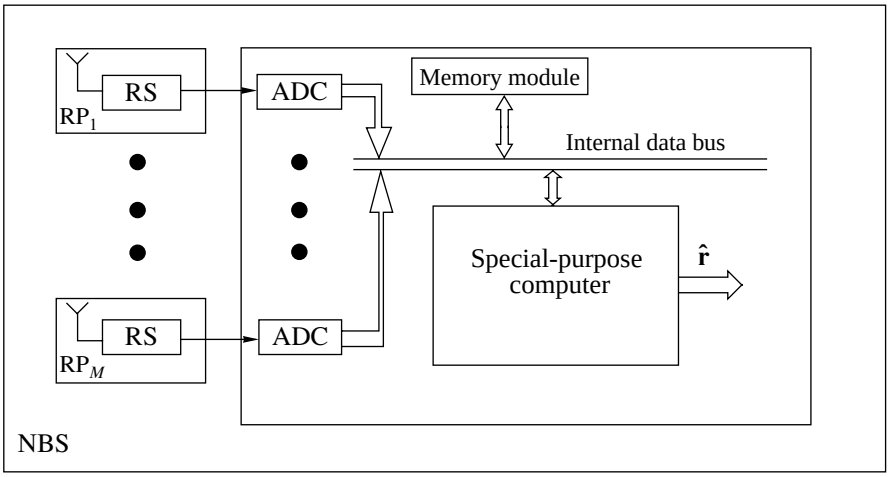

Fig. 14.

This advantage lies in the following. Rule (26) for estimating coordinates from measured bearings was derived under the assumption that bearing measurement errors have normal distribution. This assumption is valid for large signal-to-noise ratios. If the signal level falls, the distribution law of the bearing measurement errors increasingly deviates from the normal law. Consequently, algorithm (26) ceases to be optimal. The loss in the accuracy of determined radiator coordinates becomes the most substantial upon the appearance of abnormal errors in values of measured bearings.

The cause of the advantage of the one-stage algorithm over the direction-finding one is additionally explained in Figs. 9–13. These figures depict lines of equal values of the LFs of the one-stage algorithm plotted as functions of coordinates x and y for different values of the signal-to-noise ratio (concentric lines around the small circle with a cross marking the radiator position measured with the one-stage method) and bearing lines formed by the direction-finding algorithm (rays going out from measuring sites). Crosses in the figures mark lines of equal values of the LF for which these values are presented in the figure. The triangle with the letter R marks the true position of the radiator. Each figure shows the pattern of a single observation of the radiator from five aforementioned sites. Values of LFs for different x and y were calculated using formula (12). Components of vector **a** (required in formula (12)) were determined from formula (33). For each site, the bearing was estimated in accordance with formula (31).

Analyzing Figs. 9–13, we can notice that, at signal-to-noise ratios less than 0 dB, the direction-finding system operates increasingly worse because abnormal errors may arbitrarily "turn" the measured direction to the radiator. Therefore, attempts to improve the quality of measured coordinates by using acquisition of the bearing information and well-known algorithms similar to algorithm (26) cannot give the desired result. We can propose several procedures that select (ignore) abnormal bearing measurements. In this case, the reference method for operation of a position-finding system is the one-stage method for measuring the radiator coordinates and heuristic procedures derived from some reasoning should be compared with the one-stage algorithm in order to estimate the loss in the coordinate measurement accuracy.

As to the practical implementation, the differences between the one-stage and two-stage (direction-finding) systems mainly lie in the software. As a possible design version of the aforementioned systems, Fig. 14 shows the general block diagram of a coordinate meter installed onboard a carrier moving in space. The meter contains M reception points, M analog-to-digital converters (ADCs), a special-purpose computer, and peripheral devices required for operation of the above components (memory modules, internal data bus, etc.). This structure of the measuring system allows the implementation of both one-stage algorithm (14) and two-stage algorithm described by relationships (22) and (26). The implementation will be ensured by the special-purpose computer, which can run the code of the chosen measurement algorithm.

7. CONCLUSIONS

Using the maximum likelihood method, we obtained the one-stage algorithm for estimation of the radiator position by a passive system consisting of narrow-base subsystems. The proposed one-stage position-finding system can be implemented on the basis of one carrier moving in space. Expenses of the hardware of the two-stage (direction-finding) and the one-stage systems are almost equal.

Analysis of the one-stage and two-stage (direction-finding) algorithms revealed that, in both cases, accuracies of coordinate measurements are identical if the signal-to-noise ratio exceeds some threshold level ensuring normal operation of the direction-finding algorithm. However, determining coordinates of weak signal sources (when powers of received signals are comparable to noise), it is expedient to use the one-stage algorithm offering a lower value of the signal-to-noise threshold.

REFERENCES

1. A. V. Dubrovin and Yu. G. Sosulin, Radiotekh. Élektron. (Moscow) **43**, 1486 (1998) [J. Commun. Technol. Electron. **43**, 1388 (1998)].
2. V. I. Tikhonov, *Statistical Radio Engineering* (Radio i Svyaz', Moscow, 1982) [in Russian].
3. G. A. Korn and T. M. Korn, *Mathematical Handbook for Scientists and Engineers: Definitions, Theorems, and Formulas for Reference and Review*, 2nd enl. and rev. ed. (McGraw-Hill, New York, 1968; Nauka, Moscow, 1984).
4. V. P. Denisov, Radiotekh. Élektron. (Moscow) **23**, 1631 (1978).
5. D. J. Torriery, IEEE Trans. Aerosp. Electron. Syst. **20**, 183 (1984).
6. Ya. D. Shirman and V. N. Manzhos, *Theory and Technique of Radar Data Processing in the Presence of Interferences* (Radio i Svyaz', Moscow, 1981).